[8]R. E. Allen, G. P. Alldredge, and F. W. de Wette, Phys. Rev. B 4, 1648 (1971).
[9]M. Hass, Phys. Rev. Letters 13, 429 (1964).
[10]R. Englman and R. Ruppin, *Light Scattering Spectra of Solids*, edited by G. B. Wright (Springer, New York, 1969).
[11]M. Hass and H. B. Rosenstock, Appl. Opt. 6, 2079 (1967).

PHYSICAL REVIEW B VOLUME 5, NUMBER 10 15 MAY 1972

Structure of Orthorhombic $V_{0.95}Cr_{0.05}O_2$ †

J. W. Pierce and J. B. Goodenough
Lincoln Laboratory, Massachusetts Institute of Technology, Lexington, Massachusetts 02173
(Received 15 July 1971)

A structure determination of the orthorhombic phase of $V_{0.95}Cr_{0.05}O_2$ based on powder data indicates that the probable space group is $F222$ and the room-temperature lattice parameters are $a_o = 13.015$ Å, $b_o = 12.597$ Å, and $c_o = 5.795$ Å. The structure represents a distortion of the tetragonal rutile structure of high-temperature ($T > 68$ °C) V_2O_4 having cell parameters $a_r \approx a_0/2\sqrt{2} \approx b_o/2\sqrt{2}$ and $c_r \approx \frac{1}{2}c_o$. The orthorhombic cell contains $16(V_{0.95}Cr_{0.05})_2O_4$. There are four distinguishable c-axis chains of edge-shared octahedra: Cations V_1 in $4a$ and V_2 in $4b$ occupy alternate positions of one chain, the V_1-O separations being nearly uniform (≈ 1.895 Å), whereas the V_2-O distances along b_o are shorter (1.85 Å) and the four others are longer (2.04 Å). Cations V_3 in $8j$ and V_4 in $8i$ exhibit antiferroelectric displacements along half the c-axis chains, and cations V_5 form V_5-V_5 pairs along the fourth c-axis chain. The relationship of this structure to the semiconductor-to-metal transition in VO_2 is discussed.

I. INTRODUCTION

In a previous paper[1] it has been argued that the monoclinic-to-tetragonal transition in VO_2 at 340 K consists of two distinguishable components: an antiferroelectric-to-paraelectric transition and a simultaneous change from homopolar bonding of V-V pairs to metallic bonding within a V^{4+} ion chain along the monoclinic axis $a_m \approx 2c_r$, which is parallel to the tetragonal c_r axis. The two transitions, monoclinic-to-orthorhombic at T_t' and orthorhombic-to-tetragonal at T_t, that have been reported[2] for the system $V_{1-x}Cr_xO_2$ were therefore interpreted to signal the separation of these two components. According to this interpretation, the orthorhombic phase appearing in the intermediate temperature range $T_t' < T < T_t$ should manifest primarily—if not purely—antiferroelectric-type displacements of the V^{4+} ions from the centers of symmetry of their octahedral sites. In order to check this hypothesis, the orthorhombic room-temperature structure of $V_{0.95}Cr_{0.05}O_2$ has been determined from intensity measurements of an x-ray powder diffraction pattern.

II. EXPERIMENTAL

The powder material used in this study was prepared by firing V_2O_3, V_2O_5, and CrO_2 for five days at 700 °C in an open platinum bullet that had been sealed in an evacuated quartz tube. The V_2O_3 was prepared by hydrogen reduction of Johnson Mathey V_2O_5, and the CrO_2 was obtained by decomposition of CrO_3 at 20 kbar and 400 °C.[3]

Positions of the diffraction peaks were obtained from a $\frac{1}{4}$°/min diffractometer scan using a Norelco goniometer and monochromated (graphite crystal) Cu $K\alpha$ radiation. These were corrected by calibration against a silicon external standard. Lattice parameters were obtained by refinement of 2θ values using the simplex method. Observed d spacings and those calculated from the refined lattice parameters are listed for comparison in Table I.

Intensity data were collected on a Norelco diffractometer by accumulating counts while scanning over the peak, or group of peaks, at $\frac{1}{4}$°/min and subtracting background. The value of background at a particular 2θ value was taken from a curve constructed from background regions containing no peaks.

Refinement of variable atomic-position parameters and the cell temperature factor was made using a simplex program that minimized the discrepancy factor

$$R = 100 \sum_i |I_i^{\text{calc}} - I_i^{\text{obs}}| / \sum_i I_i^{\text{obs}} \quad .$$

The atomic scattering factors for V^{3+} and O^{2-} ions were those of Cromer and Waber,[4] while the real and imaginary parts of the anomalous dispersion terms were taken from Cromer.[5] The intensity data were corrected for polarization due to the curved, graphite diffracted-beam monochromator.

TABLE I. Observed and calculated intensities for $V_{0.95}Cr_{0.05}O_2$.

I_{obs}	I_{calc}	hkl	d_{calc}	d_{obs}	I_{obs}	I_{calc}	hkl	d_{calc}	d_{obs}
		200	6.507	···			513	1.540	1.541
2.0	0.62	020	6.298	···	20.0	23.64	280	1.530	···
		111	4.881	···			153	1.522	1.522
2.0	2.70	220	4.526	···	9.7	11.46	642	1.521	
49.3	55.41	311	3.348	3.350			660	1.509	···
					2.0	1.19	462	1.507	···
2.0	2.50	131	3.290	···					
886.3	890.65	400	3.254	3.252			533	1.455	1.455
							004	1.449	1.449
893.0	869.00	040	3.142	3.147	220.1	221.12	751		
							353	1.445	1.446
		002	2.898	···			840		
2.0	2.03	420	2.891	···					
		240	2.835	···	6.6	1.75	571	1.434	1.435
88.8	70.73	331	2.676	2.676			802	1.419	···
							480	1.417	1.417
		202	2.647	···	67.9	82.28	204	1.414	···
2.0	1.71	022	2.632	···			024	1.412	···
868.0	872.09	222	2.440	2.439					
					7.5	7.03	911	1.394	1.394
17.9	17.98	511	2.333	2.333					
							822	1.384	1.384
		151	2.275	···	3.1	6.47	082		
94.6	101.34	440	2.263	2.262			224	1.380	1.380
2.0	1.47	600	2.169	···					
					2.0	0.31	282	1.353	···
195.6	196.78	402	2.164	2.164			191		
209.8	182.13	042	2.132	2.132			662	1.338	1.338
					276.2	272.58	713	1.332	
2.0	0.03	060	2.099	···			931	1.331	
		531	2.067	···					
		620	2.051	···			404	1.324	1.324
45.4	45.60	422	2.047	2.048	151.4	152.12	553	1.321	···
		351	2.039	···			044	1.316	1.316
		242	2.026	···			173	1.310	···
					2.0	4.75	1000	1.301	···
37.1	48.25	260	1.998	1.998					
							391	1.298	
30.1	18.94	113	1.889	1.890			424	1.295	
					13.3	9.13	842	1.293	1.293
		640	1.786	···			244	1.290	
2.0	1.95	442	1.783	···			860	1.286	
		460	1.764	···					
							733	1.276	
		711	1.753	1.753			1020	1.275	
36.1	34.39	313	1.748	···	28.5	21.68	680		1.273
							482	1.273	
		133	1.739	···					
26.2	28.03	602	1.737	1.736			771	1.262	1.262
		551	1.728	···	13.0	7.87	373	1.260	···
							0100		···
		171	1.704	···					
2.0	0.27	062	1.700	···			2100	1.237	
					4.1	6.98	951	1.226	1.230
429.4	431.58	622	1.674	1.674					
					19.6	28.49	444	1.220	1.220
499.6	468.24	262	1.645	1.645					
							591	1.206	···
		731	1.631	1.631			604		···
134.2	168.14	333	1.627	1.627			1040	1.203	···
		800			2.0	6.79	064	1.192	···
							1002	1.187	···
6.6	14.45	371	1.598	1.599					
							624	1.183	1.184
		820	1.575	1.575	5.4	6.26	753		
152.9	150.52	080							

TABLE I. (*Continued*)

I_{obs}	I_{calc}	*hkl*	d_{calc}	d_{obs}	I_{obs}	I_{calc}	*hkl*	d_{calc}	d_{obs}
		862	1.175	...	2.0	6.71	791	1.098	...
10.6	11.21	573		1.175			393	1.097	...
		4$\underline{1}$00					6$\underline{1}$00	1.089	...
		264	1.173	...	3.1	7.64	4$\underline{1}$02		1.088
12.5	22.40	1$\underline{0}$22	1.167	1.167			3$\underline{1}$11	1.088	...
		682					1$\underline{2}$00	1.085	
		01$\underline{0}$2	1.155		64.7	67.49	335	1.082	1.082
		1$\underline{1}$11					804		
41.3	21.48	913	1.153	1.153					
		115	1.150		2.0	2.71	773	1.075	...
							1$\underline{2}$20	1.069	...
		21$\underline{0}$2	1.137	1.137					
90.6	84.71	880	1.131	1.132	45.4	50.42	824	1.066	1.065
		193	1.129	1.128			084		
							2$\underline{1}$20	1.036	
2.0	0.00	644	1.125	...	22.3	33.51	1$\underline{0}$62	1.033	1.034
		971	1.107	1.109			5$\underline{1}$11	1.031	
21.0	15.13	1$\underline{0}$60							
					18.7	19.60	4$\underline{1}$20	0.999	0.9992
							8$\underline{1}$00	0.906	

III. RESULTS

Chamberland[6] has shown that the powder patterns of a number of cation-substituted VO_2 phases can be indexed on the basis of an orthorhombic cell of either *Fmmm*, *Fmm*2, or *F*222 symmetry. Our sample of composition $V_{0.95}Cr_{0.05}O_2$ had the orthorhombic lattice parameters $a_o = 13.015$ Å, $b_o = 12.597$ Å, and $c_o = 5.795$ Å at room temperature (see Appendix). The systematic extinctions were consistent with a face-centered cell, and subsequent refinement indicated that the probable space group is *F*222.

Three observations suggested that the orthorhombic structure, like the monoclinic structure of VO_2, is closely related to the tetragonal rutile structure of high-temperature VO_2: (i) the existence of the rutile structure at $T > T_t$ (space group $P4_2/mnm$; $a_r = 4.5534$ Å, $c_r = 2.8502$ Å for VO_2),[7] (ii) the derivation of the low-temperature ($T < T_t'$) forms from the rutile structure, and (iii) similarities in the three powder patterns. In addition, the orthorhombic and tetragonal axes are related as $a_o \approx b_o \approx 2\sqrt{2}\,a_r$ and $c_o \approx 2c_r$. Therefore the observed orthorhombic cell was superimposed on the rutile lattice so that its long axes lay along the diagonals of the rutile cell, as illustrated in Fig. 1. Models were then derived by assigning the thirty-two vanadium and sixty-four oxygen atoms in the cell to positions consistent with each of the three possible space groups (*Fmmm*, *Fmm*2, *F*222) and small displacements from the tetragonal lattice positions.

Refinement in space group *F*222 using the sixty intensities listed in Table I gave the cell temperature factor and thirteen variable position parameters of Table II with a reliability factor $R = 6.0\%$.

Sixteen peaks, or composite peaks, having zero observed intensity were assigned an intensity equal to half that of the minimum peak in the pattern and were included in the refinement. There were no outstanding discrepancies among these peaks. However, removing their contribution to the refined reliability factor gave a value $R = 5.6\%$. It should be noted that the data used in the refinement include all of the peaks allowed by the space group *F*222 over the range $12° < 2\theta < 102°$, with the exception of two low-intensity envelopes containing contributions from seven or more allowed peaks.

The model consistent with space group *Fmmm* allowed seven variable position parameters and

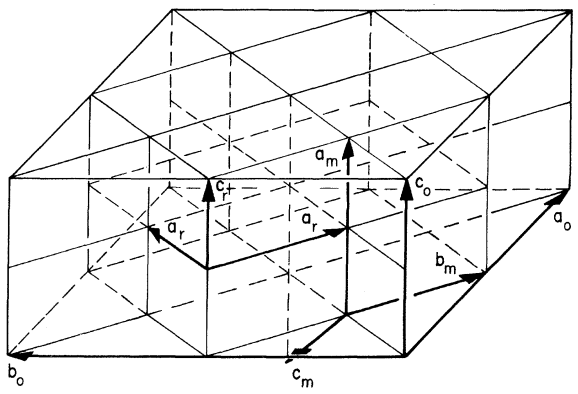

FIG. 1. Relationship of tetragonal and monoclinic phases to the orthorhombic phase in interval $T_t' < T < T_t$ of $V_{0.95}Cr_{0.05}O_2$.

was refined on the same data to a reliability factor $R = 15.7\%$. The high R factor obtained was the basis for the rejection of this model. A similar refinement of the twenty-one variable position parameters allowed by space group $Fmm2$ converged to a reliability factor $R = 6.3\%$. The fact that the R factor increased in spite of the increase in the number of parameters indicates that this model is unsatisfactory in comparison to that of $F222$.

The above observations are regarded as a clear indication that the most probable space group is $F222$.

IV. DISCUSSION

Figure 2 illustrates the atomic displacements responsible for the change from tetragonal to orthorhombic symmetry. The orthorhombic structure contains four distinguishable chains of edge-shared octahedral sites parallel to the c_o axis. One chain contains the two distinguishable cations V_1 and V_2, which remain in the center of symmetry of their respective octahedral sites. The O_1 ions in an a_o-c_o plane are displaced toward the V_1 ions and away from the V_2 ions; they are also rotated about their nearest V_1-V_2 axis. The second chain consists of alternating V_3 and $V_{3'}$ ions, which are oppositely displaced along the orthorhombic a_o axis to make very short V_3-O_5 bonds: The V_3-O_5 separation is 1.68 Å, whereas the V_3-O_6 separation is 2.20 Å. The third chain also consists of oppositely displaced V_4 and $V_{4'}$ ions, but along the orthorhombic b_o axis to make two shortest V_4-O_2 bonds of 1.87 Å. Only the fourth chain consists of V-V pairs along the c_o axis. The bridging O_6 ions between the V_5-$V_{5'}$ pairs have a V_5-O_6 separation of only 1.84 Å.

Analysis of the principal driving force responsible for this structure must begin with a definition of cooperative ferroelectric-type displacements, which create preferential metal-anion bonds. The phenomenological definition in terms of vibration-mode softening, although descriptively useful, provides no insight as to why a particular mode, or set of modes, becomes soft. For this latter purpose, we must consider the electronic energies, since the internal energy is the sum of all the one-electron energies. As there are no localized $3d$ electrons in VO_2,[1] we need consider only itinerant electrons in band or molecular-orbital states.

The compound $SrVO_3$ has the cubic perovskite structure and is reported to be metallic and Pauli paramagnetic.[8] This demonstrates that the V^{4+}-O^{2-}: p_π-V^{4+} interactions are strong enough to delocalize the single $3d$ electron per V^{4+} ion in this compound.[9] (The formal valence V^{4+} indicates the number of "$3d$" electrons per cation, since the Fermi energy lies between a filled O^{2-}: $2p$ valence band and an empty V: $4s$ conduction band.) Qualitatively, the band structure for this compound would be similar to that for ReO_3, the Sr^{2+} ions donating two electrons per cation to the $(VO_3)^{2-}$ array. This band structure, in the absence of spin-orbit coupling, would be like that shown schematically in Fig. 3.

Let us assume that at low temperatures $SrVO_3$ undergoes an antiferroelectric distortion to tetragonal symmetry, the V^{4+} ions along any tetragonal c_t axis being displaced away from one near-neighbor anion on this axis toward another. Such a displacement would be similar to the displacement of the V_3 ions in $V_{0.95}Cr_{0.05}O_2$ to form one short V_3-O_5 bond and one long V_3-O_6 bond. Ferroelectric displacements along the tetragonal [001] axis, but antiferroelectric displacements within the (001) planes, would lead to a tetragonal, antiferroelectric phase. Such a distortion would remove the threefold degeneracy (spin-orbit coupling neglected) of the π^* band, raising the bands formed from $d_{yz}d_{zx}$ orbitals relative to those formed from d_{xy} orbitals, where the z axis is taken parallel to c_t. The energies of the $d_{yz}d_{zx}$ orbitals would be raised because the atomic displacement would increase the covalent mixing between these orbitals and the nearest-neighbor anion p_yp_x orbitals, thereby destabilizing the antibonding $d_{yz}d_{zx}$ orbitals and stabilizing the anion p_yp_x orbitals. The increase ΔE_g in the splitting between $d_{yz}d_{zx}$ and p_xp_y orbitals would be proportional to the magnitude δ of the atomic displacements. In general, the number of states stabilized in the bonding π band is proportional to $(E_g+\Delta E_g)/(W_b+\frac{1}{2}E_g) = A + B\delta + \cdots$, where W_b is the width of the π band. Since the elastic restoring forces vary as δ^2, a finite displacement of the cations can be anticipated at low temperatures if the destabilized, antibonding π^* band states are empty, the elastic restoring forces are relatively small (i.e., the V^{4+} ion is small for its octahedral interstice), and $W_b/E_g \lesssim 1$. Ferroelectric-type displacements are common where the d orbitals are empty. Although a V^{4+} ion has one $3d$ electron, a finite displacement that is large enough to raise the $d_{yz}d_{zx}$ bands

TABLE II. Crystal structure of $V_{0.95}Cr_{0.05}O_2$.

Space group: $F222$ (No. 22)		
Unit-cell dimensions: $a = 13.015$ Å, $b = 12.597$ Å, $c = 5.795$ Å		
Cell content: $16V_2O_4$		
V_1 in (4a)	(0, 0, 0)	
V_2 in (4b)	(0, 0, $\frac{1}{2}$)	
V_3 in (8j)	(x, $\frac{1}{4}$, $\frac{1}{4}$; $\frac{1}{2}-x$, $\frac{1}{4}$, $\frac{1}{4}$)	$x = 0.0218(2)$
V_4 in (8i)	($\frac{1}{4}$, y, $\frac{1}{4}$; $\frac{1}{4}$, $\frac{1}{2}-y$, $\frac{1}{4}$)	$y = 0.0024(2)$
V_5 in (8h)	($\frac{1}{4}$, $\frac{1}{4}$, z; $\frac{1}{4}$, $\frac{1}{4}$, $\frac{1}{2}-z$)	$z = 0.0316(8)$
O_1 in (16k)	(x, y, z; x, $\bar{y}$, $\bar{z}$; $\bar{x}$, $\bar{y}$, z; $\bar{x}$, y, $\bar{z}$)	$x = 0.1020(5)$; $y = 0.0074(5)$; $z = 0.2325(10)$
O_2 in (16k)		$x = 0.2515(5)$; $y = 0.1004(5)$; $z = 0.0089(10)$
O_3 in (8f)	(0, y, 0; 0, $\bar{y}$, 0)	$y = 0.1506(5)$
O_4 in (8f)		$y = 0.3533(5)$
O_5 in (8j)	(x, $\frac{1}{4}$, $\frac{1}{4}$; $\frac{1}{2}-x$, $\frac{1}{4}$, $\frac{1}{4}$)	$x = 0.1506(5)$
O_6 in (8j)		$x = -0.1473(5)$
Cell temperature factor: 1.3		

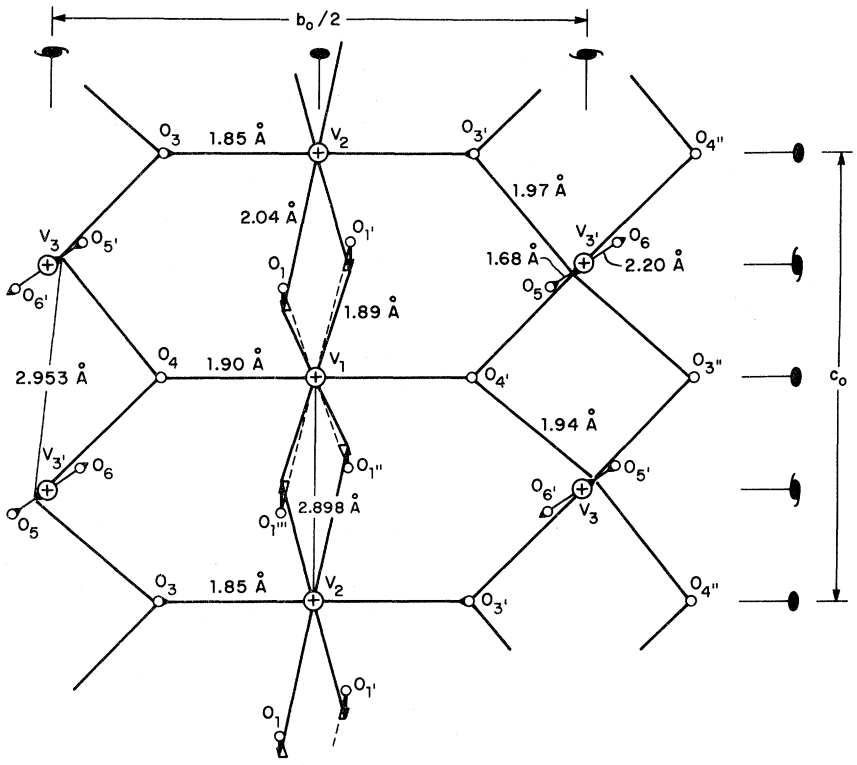

(a) ORTHORHOMBIC F222 VO_2 : Cr

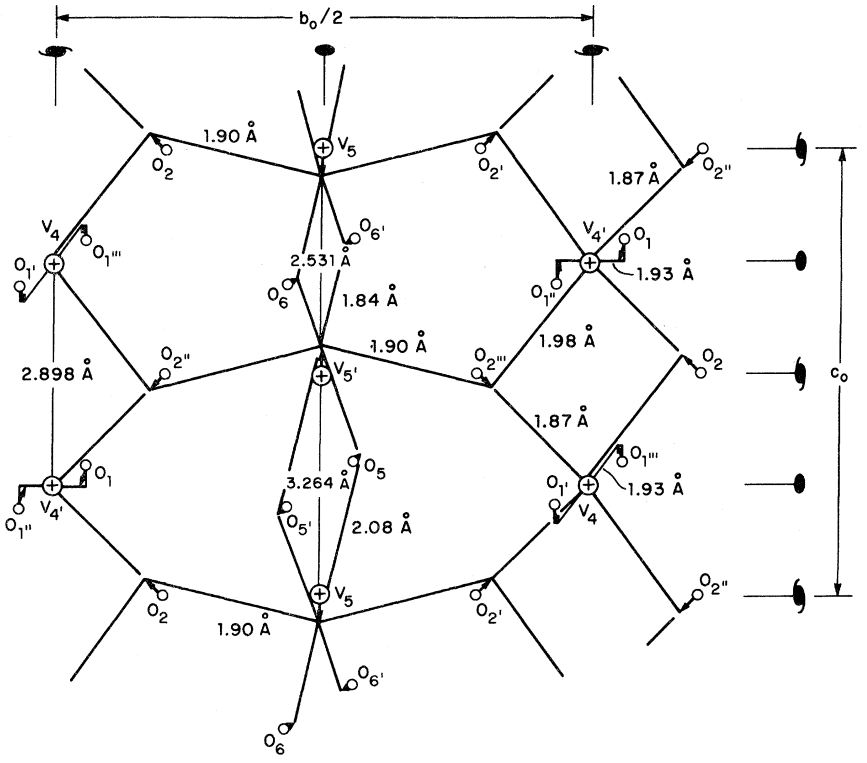

(b) ORTHORHOMBIC F222 VO_2 : Cr

FIG. 2. Structure of orthorhombic room-temperature $V_{0.95}Cr_{0.05}O_2$: anion coordination about (a) (V_1+V_2) and V_3 chains and (b) V_4 and V_5 chains of alternate b_o-c_o planes.

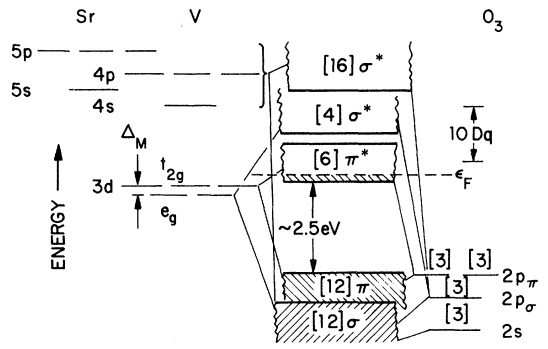

FIG. 3. Schematic one-electron band structure of $SrVO_3$ without spin-orbit coupling, after J. B. Goodenough [J. Appl. Phys. 37, 1415 (1966)] and L. F. Mattheiss [Phys. Rev. 181, 987 (1969)].

above the Fermi energy of $SrVO_3$ is theoretically possible, especially if the antiferroelectric displacements, which increase the size of the unit cell in the basal planes, simultaneously split the d_{xy} band to stabilize occupied d_{xy} states relative to unoccupied d_{xy} states. In this latter case, the antiferroelectric phase change would be accompanied by a metal-to-semiconductor transition with decreasing temperature. The apparent lack of a spontaneous distortion in $SrVO_3$ is probably due to the breadth of the π^* band and the fact that such a distortion would tend to quench any stabilization due to spin-orbit coupling.

In the rutile structure of tetragonal VO_2, each anion has three near-neighbor cations in the same plane, and the anion p orbital perpendicular to this plane is a p_π orbital available for π bonding with cation d orbitals. In the metallic, tetragonal phase of VO_2, the occupied $3d$ bands consist of pseudodegenerate π^* bands and a $d_\parallel$ band having a_{1g} symmetry at Γ, the center of the Brillouin zone, as shown in Fig. 4(a). In the monoclinic, low-temperature phase an antiferroelectric displacement of the cations lifts the π^* bands above the Fermi energy, and a V-V pairing along the tetragonal [001] axis splits the $d_\parallel$ band in two, as shown in Fig. 4(b).[1] Therefore a semiconductor-to-metal transition accompanies the phase transformation with increasing temperature. That such a transition has been found in VO_2, but not in $SrVO_3$, is probably due to not only the narrowness and relative stability of the $d_\parallel$ band in VO_2, but also a quenching of the orbital angular momentum in VO_2.

In the composition $V_{0.95}Cr_{0.05}O_2$, the chromium ion apparently holds three localized $3d$ electrons in a $^4A_{2g}$ ground-state manifold. Therefore the formal valences for the compound are $V^{4+}_{0.9}V^{5+}_{0.05}Cr^{3+}_{0.05}O_2$ where the V^{5+} ions are trapped at sites neighboring the Cr^{3+} ions. Since Cr-V bonding is not anticipated, stabilization by the cooperative V-V pairing along the tetragonal [001] axis must be reduced. On the other hand, the small V^{5+} ion, which has empty $3d$ orbitals, generally undergoes a ferroelectric-type displacement from the center of symmetry of an octahedral interstice, so that stabilization of a cooperative antiferroelectric distortion might even be increased despite lack of participation in this distortion by the Cr^{3+} ion. Therefore the appearance in $V_{0.95}Cr_{0.05}O_2$ of an orthorhombic phase in the temperature interval $T_t' < T < T_t$ was presumed[1] to signal the presence of primarily antiferroelectric displacements in this phase. The existence of V-V pairs along only one-fourth of the c_o-axis chains clearly demonstrates the anticipated suppression of V-V homopolar bonding in the orthorhombic-vs-monoclinic phases.

The existence of antiferroelectric displacements is also clearly evident for the V_3 and V_4 ions. The V_3 ions form one strong p_y-d_{xy} π bond and a weaker p_z-d_{zx} π bond with the nearest-neighbor O_5 anion. Competition with (sp_xp_z) hybridization for σ bonding weakens the second of these, so that the V_3-O_5 separation is intermediate to that found for V-O double π and single π bonds in other compounds: 1.57 and 1.76 Å, respectively.[10] This places the one $3d$ electron per V^{4+} ion at V_3 sites in $d_{z^2-y^2}$ orbitals that are probably localized, the $V_3 - V_3$ separations being $R = 2.963 > 2.94$ Å $\approx R_c$ (the estimated critical separation for localized vs itinerant $3d$ electrons at V^{4+} ions in oxides[11]). Electron localization would split the $d_{z^2-y^2}$ bands by the electrostatic energy U responsible for correlating one $3d$ electron per V^{4+} ion at a V_3 site.

Each O_2 ion shares its p_π orbital with a $(d_{xy} \pm id_{zx})$ orbital at a nearest-neighbor V_4 ion and a d_{xy} orbital at a V_5 ion, so that the V_4-O_2 and V_5-O_2 distances are intermediate between single π-bond and no π-bond values: 1.76 and 1.91 Å, respectively.[10] A $d_{z^2-y^2}$ band associated with a V_4 chain ($R = 2.9$ Å $< R_c$) would be split in two by the antiferroelectric configuration along the chain.

Although the formation of V_5-V_5, homopolar-bonded pairs splits the half-filled $d_{z^2-x^2}$ band in two,

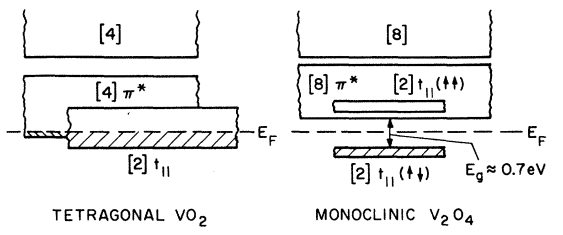

FIG. 4. Schematic modification of d-band structure of VO_2 on passing from metallic to semiconducting phase, after Ref. 1.

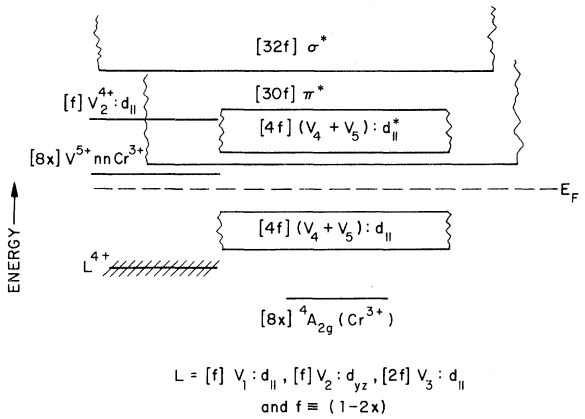

FIG. 5. Schematic d-band structure of orthorhombic $8V_{0.95}Cr_{0.05}O_2$, where $x = 0.05$ and levels associated with a formal valence state represent a localized orbital or d-state manifold.

the d_{yz} and d_{xy} orbitals π bond with two O_6 ions and two O_2 ions, thereby destabilizing these π^* orbitals to energies above the Fermi energy. The V_5-O_6 and V_5-O_2 distances of 1.84 and 1.90 Å, respectively, are intermediate between single π-bond and zero π-bond values, like the V_4-O_2 distances, because each cation orbital shares its π bonding with two anions and each anion p_π orbital shares its π bonding with two cations. Similarly, the V_2 cation shares its d_{xy} orbital with two O_3 ions, and the V_1 cation shares its d_{yz} and d_{xy} orbitals with two O_4 ions and four O_1 ions to form a nearly octahedral interstice. This leaves the single d electron per V^{4+} ion of the $V_1 + V_2$ chains in V_1: $d_{z^2-x^2}$ and V_2: ($d_{z^2-x^2}$, d_{yz}) orbitals. The difference in potential at V_1 and V_2 would split the $d_{z^2-x^2}$ band in two, thereby localizing the single electron per V^{4+} ion at V_1 in a $d_{z^2-x^2}$ orbital and the single electron per V^{4+} ion at V_2 in a d_{yz} orbital.

In summary, all of the V-O separations can be consistently correlated with enhanced π bonding that would raise the π^* bands above the Fermi energy: only the V_2: d_{yz} orbitals are an exception, and these appear to be occupied by one localized electron. Furthermore, doubling of the c axis ($c_0 \approx 2c_r$) splits the $d_{\|}$ bands in two, thereby making the orthorhombic phase a semiconductor. Finally, half of the $3d$ electrons appear to be localized: those in the ($V_1 + V_2$) chains and the $d_{\|}$ electrons at the V_3 ions. This leads to the schematic band scheme of Fig. 5, which is to be compared to those of Fig. 4. It also means that the magnetic susceptibility should be intermediate between the low value found in monoclinic VO_2, where all $d_{\|}$ electrons are spin-paired in homopolar bonds, and the exchange-enhanced value of metallic, tetragonal VO_2. Kosuge[12] first reported just such an intermediate susceptibility in the orthorhombic phase of $V_{1-x}Fe_xO_2$ samples, and Mitsuishi[13] first noted that

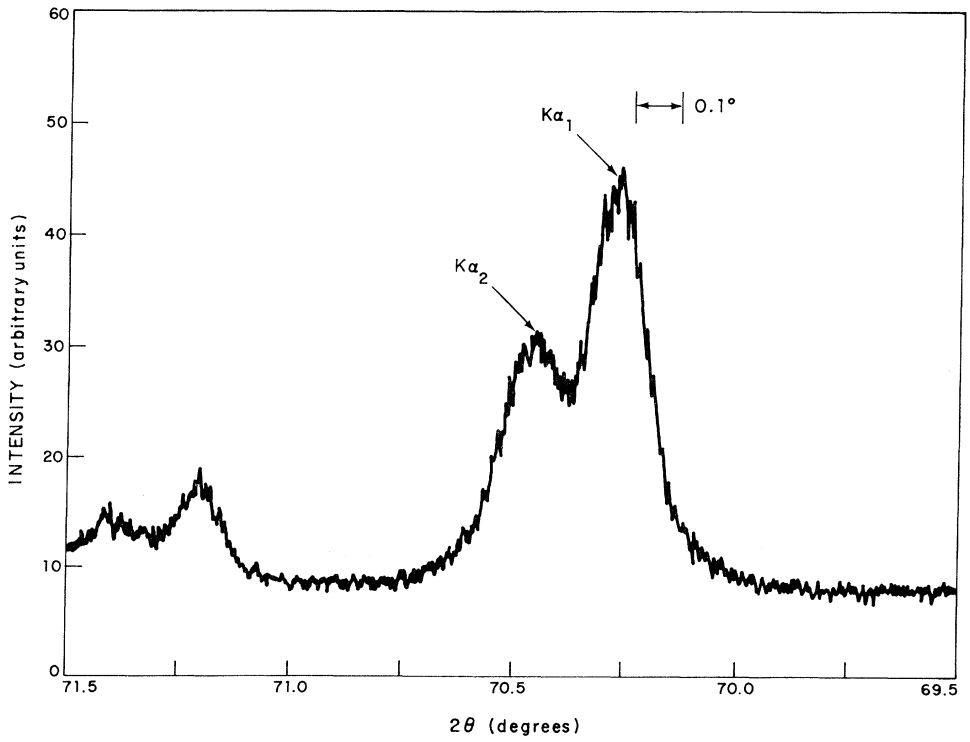

FIG. 6. Trace of x-ray diffraction pattern near $2\theta = 70°$ for powdered $V_{0.95}Cr_{0.05}O_2$.

a semiconductor-to-metal transition is associated with the orthohombic-to-tetragonal phase change at T_t.

In conclusion, the structure of orthorhombic $V_{0.95}M^{3+}_{0.05}O_2$, although somewhat more complex than anticipated in Ref. 1, is quite consistent with the argument presented there. However, this structure is not the only intermediate phase encountered in the system $V_{1-x}M^{3+}_x O_2$. The Bordeaux group[2] has observed, in a sample with $x = 0.1$, an orthorhombic structure without a doubling of the rutile c axis. Clearly there can be no V-V pairing along the c axis in this phase. There can be only ferroelectric displacements within any one chain. Marezio *et al.*[14] have reported a monoclinic phase for $x = 0.024$ in which half the chains had V-V pairing and half had antiferroelectric displacements of the vanadium ions. It would be interesting to know whether, at smaller x, there is lesser suppression of V-V pairing. It is also important to establish the role of oxygen content in the stabilization of these intermediate phases.

ACKNOWLEDGMENTS

The authors would like to thank H. Y-P. Hong for the Weissenberg study on our sample and R. J. Arnott for a helpful discussion concerning the structure refinement.

APPENDIX

After this paper was submitted, our attention was called to a recent single-crystal study[14] of "nominal" $V_{0.976}Cr_{0.024}O_2$. This crystal was monoclinic, space group $C2/m$. Its powder pattern was remarkably similar to that of the orthorhombic phase reported here. It was distinguished from our orthorhombic phase with the aid of Guinier photographs, which showed a clearly resolved doublet in the vicinity of $d = 1.338$ Å. In view of this report, it became incumbent upon us to establish that our phase was indeed orthorhombic and not monoclinic.

Figure 6 is a trace of the single peak that we observe with the α_1 and α_2 contributions (separation $\sim 0.2°$) clearly resolved. It shows no sign of splitting. In addition Guinier photographs were taken, and no definite sign of splitting was observed. As a final precaution, Weissenberg photographs were taken using a single crystal selected from the powder. These photographs indicated mmm symmetry, and the measured angle between the principal axes of the monoclinic cell was $90.0° \pm 0.1°$.

---

†Work sponsored by the Department of the Air Force.

[1]J. B. Goodenough, J. Solid State Chem. 3, 490 (1971).

[2]G. Villeneuve, A. Bordet, A. Casalot, and P. Hagenmuller, Mater. Res. Bull. 6, 119 (1971).

[3]D. S. Chapin, J. A. Kafalas, and J. M. Honig, J. Phys. Chem. 69, 1402 (1965).

[4]D. I. Cromer and J. I. Waber, Acta Cryst. 18, 104 (1965).

[5]D. I. Cromer, Acta Cryst. 18, 17 (1965).

[6]B. L. Chamberland (private communication).

[7]K. V. Krishna Rao, S. V. Nagender Naidu, and L. Iyengar, J. Phys. Soc. Japan 23, 1380 (1967).

[8]M. Wollnik, thesis (Technische Universität Berlin, 1965) (unpublished); B. Reuter, Bull. Soc. Chim. France No. 4, 1053 (1965).

[9]J. B. Goodenough and J. M. Longo, *Landolt-Bornstein Tabellen Neue Serie III/4a* (Springer-Verlag, Berlin, 1970), p. 126.

[10]J. Galy, J. Darriet, A. Casalot, and J. B. Goodenough, J. Solid State Chem. 1, 339 (1970); J. B. Goodenough, *ibid.* 1, 349 (1970); in *Conduction in Low-Mobility Materials*, edited by N. Klein, D. S. Tannhauser, and M. Pollak (Taylor and Francis, London, 1971), p. 87.

[11]J. B. Goodenough, Czech. J. Phys. B17, 304 (1967).

[12]K. Kosuge, J. Phys. Soc. Japan 22, 551 (1967).

[13]T. Mitsuishi, Japan. J. Appl. Phys. 6, 1060 (1967).

[14]M. Marezio, D. B. McWhan, J. P. Remeika, and P. D. Dernier, Phys. Rev. B (to be published).